

11. Oomi, G., Kuwahara, R., Kagayama, T. & Jung, A. Pressure-induced volume anomaly of intermediate valence compound  $\text{Sm}_{0.9}\text{La}_{0.1}\text{S}$ . *J. Magn. Magn. Mater.* **226-230**, 1182–1183 (2001).
12. de Visser, A., Bakker, K. & Pierre, J. Anomalous negative thermal expansion of  $\text{CeInCu}_2$ . *Physica B* **186-188**, 577–579 (1993).
13. Lang, M., Schefzyk, R., Steglich, F. & Grewe, N. Negative thermal expansion in the Kondo system  $\text{Ce}_{x}\text{La}_{1-x}\text{Al}_2$ . *J. Magn. Magn. Mater.* **63-64**, 79–81 (1987).
14. Hormillosa, C., Healy, S. & Stephen, T. *Valence Bond Calculator version 2.00* (I. D. Brown, Institute for Material Research, McMaster University, Hamilton, Ontario, Canada, 1993).

**Acknowledgements** Financial support from the Department of Energy is gratefully acknowledged.

**Competing interests statement** The authors declare that they have no competing financial interests.

**Correspondence** and requests for materials should be addressed to M.G.K. (kanatzid@cem.msu.edu).

## Reduction of soil carbon formation by tropospheric ozone under increased carbon dioxide levels

Wendy M. Loya<sup>1</sup>, Kurt S. Pregitzer<sup>1</sup>, Noah J. Karberg<sup>1,2</sup>, John S. King<sup>1</sup> & Christian P. Giardina<sup>1,2</sup>

<sup>1</sup>School of Forest Resources and Environmental Science, Michigan Technological University, Houghton, Michigan 49931, USA

<sup>2</sup>USDA Forest Service, North Central Research Station, Houghton, Michigan 49931, USA

In the Northern Hemisphere, ozone levels in the troposphere have increased by 35 per cent over the past century<sup>1</sup>, with detrimental impacts on forest<sup>2,3</sup> and agricultural<sup>4</sup> productivity, even when forest productivity has been stimulated by increased carbon dioxide levels<sup>5</sup>. In addition to reducing productivity, increased tropospheric ozone levels could alter terrestrial carbon cycling by lowering the quantity and quality of carbon inputs to soils. However, the influence of elevated ozone levels on soil carbon formation and decomposition are unknown. Here we examine the effects of elevated ozone levels on the formation rates of total and decay-resistant acid-insoluble soil carbon under conditions of elevated carbon dioxide levels in experimental aspen (*Populus tremuloides*) stands and mixed aspen–birch (*Betula papyrifera*) stands. With ambient concentrations of ozone and carbon dioxide both raised by 50 per cent, we find that the formation rates of total and acid-insoluble soil carbon are reduced by 50 per cent relative to the amounts entering the soil when the forests were exposed to increased carbon dioxide alone. Our results suggest that, in a world with elevated atmospheric carbon dioxide concentrations, global-scale reductions in plant productivity due to elevated ozone levels will also lower soil carbon formation rates significantly.

Table 1 Total carbon and  $\delta^{13}\text{C}$  of soils and the acid-insoluble fraction

	Total soil carbon		Acid-insoluble fraction	
	Total C ( $\text{g m}^{-2}$ )	$\delta^{13}\text{C}$ (‰)	Total C ( $\text{g m}^{-2}$ )	$\delta^{13}\text{C}$ (‰)
Control	5,385 ± 241	-26.7 ± 0.11	2,287 ± 185	-27.7 ± 0.06
Elevated $\text{O}_3$	5,237 ± 72	-26.9 ± 0.06	2,671 ± 224	-27.7 ± 0.11
Elevated $\text{CO}_2$	5,683 ± 480	-28.3 ± 0.10	2,594 ± 230	-29.0 ± 0.12
Elevated $\text{O}_3 + \text{CO}_2$	5,114 ± 369	-27.6 ± 0.10	2,473 ± 97	-28.5 ± 0.10

Determined for mineral soil from 0 to 20 cm. Values are mean ± s.e.

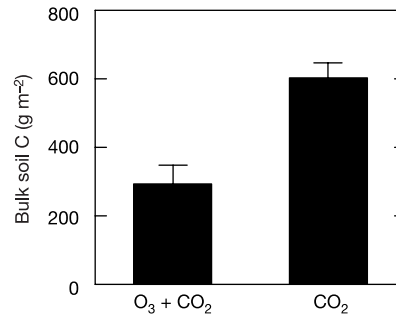


Figure 1 Total carbon incorporated into soils during 4 yr of exposure to elevated  $\text{O}_3 + \text{CO}_2$  and elevated  $\text{CO}_2$ . Values are mean ± 1 s.e.;  $P < 0.01$ .

Large areas of the Earth are exposed to concentrations of tropospheric ozone ( $\text{O}_3$ ) that exceed levels known to be toxic to plants<sup>4,6</sup>. In addition to reducing plant growth, exposure to elevated  $\text{O}_3$  can also alter plant tissue chemistry<sup>7</sup> and reduce allocation of carbon to roots and root exudates<sup>8–10</sup>. Whereas the effects of  $\text{O}_3$  on these aspects of plant biology have been widely investigated in chamber studies, examination of these effects on below-ground carbon cycling in intact forests only became possible in 1997 with the establishment of the FACTS-II (forest–atmosphere carbon transfer and storage) FACE (free-air carbon dioxide enrichment) experiment in Rhinelander, Wisconsin, USA. The long-term FACE experiment in Rhinelander examines how plant–plant and plant–microbe interactions may alter ecosystem responses to elevated  $\text{O}_3$  and carbon dioxide ( $\text{CO}_2$ ) through four treatments: control, elevated  $\text{CO}_2$ , elevated  $\text{O}_3$  and elevated  $\text{O}_3 + \text{CO}_2$ . In plots where  $\text{O}_3$  and  $\text{CO}_2$  are elevated, concentrations were maintained at ~150% of ambient levels<sup>11</sup>. To examine the effects of atmospheric trace gases on both ecological interactions and on whole-ecosystem carbon cycling, each plot is split to include a pure aspen forest, a mixed aspen–birch forest and a mixed aspen–maple forest. These species were chosen because they are among the most widely distributed trees in northern temperate forests.

Here we compare soil carbon formation in aspen and aspen–birch subplots under elevated  $\text{CO}_2$  and elevated  $\text{O}_3 + \text{CO}_2$  (three plots each) to understand how exposure to  $\text{O}_3$  under elevated  $\text{CO}_2$  alters soil carbon formation. We used  $\text{CO}_2$  derived from fossil fuel with its highly depleted  $^{13}\text{C}$  signature to fumigate plant canopies in the elevated  $\text{CO}_2$  and elevated  $\text{O}_3 + \text{CO}_2$  plots. Leaf and root carbon inputs in the elevated  $\text{CO}_2$  and elevated  $\text{O}_3 + \text{CO}_2$  plots had a  $\delta^{13}\text{C}$  signature of  $-41.6 \pm 0.4\text{‰}$  (mean ± s.e.) in contrast to leaf and root inputs of  $-27.6 \pm 0.3\text{‰}$  in the control plots. The  $\delta^{13}\text{C}$  signature of soil carbon was  $-26.7 \pm 0.2\text{‰}$  before fumigation and

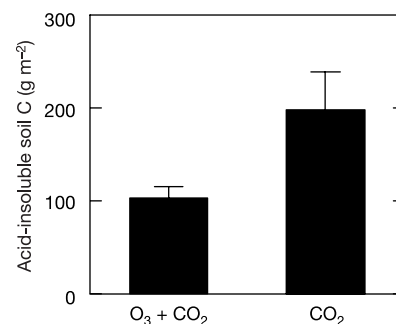


Figure 2 Carbon incorporated into the stable acid-insoluble fraction of soils during 4 yr of exposure to elevated  $\text{O}_3 + \text{CO}_2$  and elevated  $\text{CO}_2$ . Values are mean ± 1 s.e.;  $P < 0.01$ .

Table 2 Quantity and relative proportion of total soil carbon and soil carbon pools lost via microbial respiration in laboratory incubations

	Total carbon		Fumigation carbon		Pre-fumigation carbon	
	Cumulative loss	Relative mass loss	Cumulative loss	Relative mass loss	Cumulative loss	Relative mass loss
Control	1,372 ± 62	0.10 ± 0.01				
Elevated O <sub>3</sub>	1,392 ± 36	0.11 ± 0.00				
Elevated CO <sub>2</sub>	1,673 ± 85	0.12 ± 0.01	438 ± 23	0.27 ± 0.02	1235 ± 71	0.10 ± 0.00
Elevated O <sub>3</sub> + CO <sub>2</sub>	1,342 ± 42	0.11 ± 0.01	267 ± 26	0.42 ± 0.06	1075 ± 36	0.09 ± 0.00
P	0.09	0.22	0.04	0.10	0.31	0.17

Cumulative loss (mg CO<sub>2</sub>-C per kg soil). Relative mass loss (g CO<sub>2</sub>-C per g soil-C) determined for day 281 of incubation. Values are mean ± s.e.

in control plots. Because plant carbon inputs to the soils fumigated with elevated CO<sub>2</sub> and elevated O<sub>3</sub> + CO<sub>2</sub> were depleted in <sup>13</sup>C relative to soil carbon that existed before the experiment began, incorporation of new plant detritus into soil organic matter through time should decrease the δ<sup>13</sup>C of soil carbon. Using standard mixing models, we were able to determine the fraction of total soil carbon and acid-insoluble soil carbon derived from atmospheric CO<sub>2</sub> fixed by the trees over the 4 yr of experimental fumigation.

Elevated O<sub>3</sub> profoundly altered the <sup>13</sup>C composition of soil carbon after 4 yr of fumigation. The less depleted δ<sup>13</sup>C signature of total soil carbon from the elevated O<sub>3</sub> + CO<sub>2</sub> treatment compared to the elevated CO<sub>2</sub> treatment (Table 1; P < 0.01) indicates that less carbon entered the soil when aspen and mixed aspen–birch forests were exposed to both elevated O<sub>3</sub> and CO<sub>2</sub>. Carbon inputs to soil over 4 yr accounted for 10.7 ± 0.6% of the total soil carbon under elevated CO<sub>2</sub>, but only 5.7 ± 0.9% under elevated O<sub>3</sub> + CO<sub>2</sub>. Thus, elevated O<sub>3</sub> reduced total soil carbon formation by approximately 300 g C m<sup>-2</sup> compared to the amount formed under elevated CO<sub>2</sub> alone (Fig. 1).

Soils store carbon with both long and short turnover times, and to understand the carbon storage capacity of soils, it is necessary to partition soil carbon changes into decay-resistant and labile components. We used acid hydrolysis to isolate the most decay-resistant carbon in the soil<sup>12</sup>. The acid-insoluble soil carbon fraction contains the longest-lived compounds, and is composed primarily of aromatic humic acids and residues of phenols, lignin and lignin-associated cellulose from newer plant residues<sup>13</sup>. However, after careful removal of plant residues before hydrolysis, new carbon inputs measured in this fraction are restricted to the most decomposition-resistant compounds. Compared to elevated CO<sub>2</sub> alone, simultaneous O<sub>3</sub> and CO<sub>2</sub> fumigation greatly reduced the quantity of carbon entering the acid-insoluble fraction in both aspen and aspen–birch soils, as indicated by the less depleted δ<sup>13</sup>C signature (Table 1; P < 0.04). Carbon incorporated into the soil since the initiation of the experiment accounted for approximately 9.1 ± 0.8% of the acid-insoluble carbon fraction in the elevated CO<sub>2</sub> plots, but only 4.2 ± 0.6% in the elevated O<sub>3</sub> + CO<sub>2</sub> plots. Thus, the elevated O<sub>3</sub> treatment reduced formation of acid-insoluble soil carbon by approximately 100 g C m<sup>-2</sup> (or 48%) compared with elevated CO<sub>2</sub> alone (Fig. 2).

Soil carbon formation is a balance between detrital inputs and decomposition losses. Observed reductions in soil carbon formation in the elevated O<sub>3</sub> + CO<sub>2</sub> treatment could result from reduced inputs, increased losses, or both. Previous research at this site suggests that plant detrital inputs are reduced under elevated O<sub>3</sub> + CO<sub>2</sub> relative to elevated CO<sub>2</sub> alone<sup>5,10</sup>. To elucidate the effects of decomposition losses on soil carbon, we conducted a long-term laboratory incubation experiment. Despite greater microbial activity in soils from elevated CO<sub>2</sub> plots (Table 2), there was a strong trend of greater relative mass loss of carbon derived from fumigation in the elevated O<sub>3</sub> + CO<sub>2</sub> plots compared to the elevated CO<sub>2</sub> plots (Table 2; P < 0.1). This result suggests that the soil microbes responsible for carbon decomposition under elevated O<sub>3</sub> + CO<sub>2</sub> used a greater proportion (35%) of carbon formed since

fumigation began, leaving less of this carbon in the soil and in the acid-insoluble fraction. Possible reasons for greater consumption of recent carbon inputs include changes in microbial community composition<sup>14</sup>, microbial activity<sup>15</sup>, or carbon availability<sup>9</sup>. In turn, these below-ground changes could be driven by altered quantity and quality of detrital inputs<sup>5,10</sup>.

The atmospheric trace gases CO<sub>2</sub> and O<sub>3</sub> are known to influence photosynthesis and ecosystem productivity in opposite ways. It is now clear that their interaction has the potential to cascade through ecosystems, altering soil carbon cycling. In response to reduced detrital carbon supply<sup>5,10</sup> and increased microbial utilization, forest ecosystems exposed to both elevated O<sub>3</sub> and CO<sub>2</sub> accrued 51% less total, and 48% less acid-insoluble, soil carbon compared to ecosystems exposed only to elevated CO<sub>2</sub>. Our results suggest that changes in the formation of soil carbon induced by tropospheric O<sub>3</sub> should be explicitly considered in models of soil carbon cycling under scenarios of elevated CO<sub>2</sub>. □

## Methods

### Research area and field experiment

The FACTS-II FACE experiment in Rhineland, Wisconsin, USA (49° 40.5' N, 89° 37.5' E, 490 m elevation) includes three experimental treatments (elevated CO<sub>2</sub>, elevated O<sub>3</sub>, and elevated O<sub>3</sub> + CO<sub>2</sub>) and control plots arranged in a randomized complete block design with three replicates<sup>11</sup>. FACE technology combines a trace gas monitoring system with a delivery system composed of blowers and vertical pipes placed around the perimeter of the forest stand to elevate ambient concentrations of O<sub>3</sub> and CO<sub>2</sub> (ref. 11). Ambient levels of CO<sub>2</sub> and O<sub>3</sub> are approximately 347 μl l<sup>-1</sup> and 37 nl l<sup>-1</sup>, respectively. Elevated CO<sub>2</sub> and elevated O<sub>3</sub> treatments averaged 560 μl l<sup>-1</sup> and 52 nl l<sup>-1</sup>, respectively, since the fumigation began. The experiment was initiated in the summer of 1997 with the planting of greenhouse-propagated tree seedlings at 1 × 1 m spacing, in the following combinations within three sections of each 30-m ring: (1) aspen (*Populus tremuloides* Michx.); (2) aspen and birch (*Betula papyrifera* Marsh.); and (3) aspen and maple (*Acer saccharum* Marsh.). Fumigation began in May 1998. In this investigation we focus only on soil carbon in the aspen and aspen–birch stands. Soils were sampled in 1997 before the start of fumigation with elevated CO<sub>2</sub> and O<sub>3</sub>, and again in October 2001 when trees had grown to approximately 5 m height, forming a closed-canopy system in all but the elevated O<sub>3</sub> treatment where trees were smaller with less leaf production. Soils at the site are mixed, frigid, coarse loamy Alfic Haplorthods. The texture of the soil is sandy loam, underlain by a clay plough-layer, and then grading back into a sandy loam.

### Soil carbon fractionation

Soil cores (10 cm diameter × 20 cm deep) were collected at 10 random locations within each community type in each plot, composited by community type within each plot, sieved to remove roots and other coarse materials, and oven-dried before analysis for total soil carbon and δ<sup>13</sup>C. Subsamples (40 g) of each soil were extracted with 150 ml of deionized water overnight to remove water-soluble carbohydrates. We then removed any remaining fine organic matter on a portion of the residual soil by flotation with 1.0 M NaCl, rinsing with deionized water, and then manually removing any remaining particulate organic matter (POM) under a compound microscope at 20 × magnification. We then performed acid hydrolysis with 6 M HCl on a 2-g subsample of POM-free soil under reflux for 8 h to isolate the most decay-resistant carbon for %C and δ<sup>13</sup>C. Analyses of %C and δ<sup>13</sup>C were performed on a Costech Elemental Combustion System 4010 connected to a ThermoFinnigan ConfloIII Interface and Deltaplus Continuous Flow-Stable Isotope Ratio Mass Spectrometer (IRMS).

### Soil incubation and respiration measurements

A separate subsample of sieved root-free soil was used to determine potential carbon availability by aerobic incubation. We placed 100 g of field moist soil into microlysimeters constructed from funnels, brought soils to approximately 60% field capacity, then placed soils into 1-litre incubation jars which were placed in an incubator at 25.0 ± 0.5 °C. At intervals that increased in length over time, we measured CO<sub>2</sub> accumulation in the headspace by withdrawing 50 μl from sealed jars fitted with septa and measured the

concentration using a Varian CP-3800 gas chromatograph with a thermal conductivity detector. Rates of CO<sub>2</sub> production were calculated by dividing concentrations by the time since jars had been sealed. On the same date, we collected samples of gas from the headspace of incubation jars for determining the δ<sup>13</sup>C value of the accumulated CO<sub>2</sub>. We injected 7 ml of headspace gas into He-flushed gas-tight LabCo exetainers, which were then placed into an autosampler and analysed on a FIN-MAT Gas Bench II connected to the IRMS. Soil respiration δ<sup>13</sup>C values for control and elevated O<sub>3</sub> treatments were -25.0 ± 0.2‰ across the incubation. For soils from elevated CO<sub>2</sub>, soil respiration values initially were -30.9 ± 0.3‰ and increased to -28.8 ± 0.2‰ by day 281 of incubation. For the elevated O<sub>3</sub> + CO<sub>2</sub> treatment, values initially were -31.1 ± 0.4‰ and -28.2 ± 0.2 at day 281 of incubation.

**Stable isotope tracer, calculations and statistical analysis**

To investigate the contribution of new carbon inputs to soil and microbial respiration in the elevated CO<sub>2</sub> and elevated O<sub>3</sub> + CO<sub>2</sub> plots, we used the δ<sup>13</sup>C signature derived from the fossil-fuel fumigation gas mixed with ambient air (-18.7 ± 1.0‰ compared to -8.6 ± 0.1‰ for control and elevated O<sub>3</sub> plots). Subsequent fractionation by the plants produced leaf and root tissue with δ<sup>13</sup>C values of approximately -41.6 ± 0.4‰ in elevated CO<sub>2</sub> and elevated O<sub>3</sub> + CO<sub>2</sub> plots. Composite soil samples collected from all 12 plots before the experiment began in 1997 and from the three control plots in 2001 had similar (P = 0.47) δ<sup>13</sup>C values, averaging -26.7 ± 0.2‰. The proportional contribution of carbon derived from the fumigation gas (f) was calculated using the equation  $f = (\delta_i - \delta_o) / (\delta_i - \delta_o)$ , where δ<sub>i</sub> refers to the isotopic composition (δ<sup>13</sup>C) of the soil organic carbon or soil respiration from the fumigated (elevated CO<sub>2</sub> or elevated O<sub>3</sub> + CO<sub>2</sub>) plots, δ<sub>o</sub> is the δ<sup>13</sup>C of soil organic carbon or soil respiration from control plots, and δ<sub>i</sub> is the <sup>13</sup>C signature of the plant leaves and roots collected in 2001 from the fumigated plots, weighted equally and averaged across species as there were no significant differences found among the aspen and aspen-birch plots. We do not expect that the isotopic signature of the plants varied appreciably over the life of this experiment because fumigation was initiated when the trees were still seedlings. Because there were differences among treatments in the amount of carbon entering soils derived from fumigation (Fig. 1), we calculated the relative mass loss as the cumulative amount of carbon respired from each of these pools divided by the amount of soil carbon in that pool. Data were analysed using analysis of variance with general linear models for a split-plot randomized complete design using SAS 8.02 (Cary, North Carolina).

Received 25 February; accepted 12 September 2003; doi:10.1038/nature02047.

1. IPCC Climate Change 2001: Technical Summary (Report of the Intergovernmental Panel on Climate Change, IPCC Secretariat, Geneva, 2001).
2. Gregg, J. W., Jones, C. G. & Dawson, T. E. Urbanization effects on tree growth in the vicinity of New York City. *Nature* **424**, 183–187 (2003).
3. McLaughlin, S. B. & Downing, D. J. Interactive effects of ambient ozone and climate measured on growth of mature forest trees. *Nature* **374**, 252–254 (1995).
4. Chameides, W. L., Kasibhatla, P. S., Yienger, J. & Levy, H. I. Growth of continental-scale metro-agroplexes, regional ozone pollution, and world food production. *Science* **264**, 74–77 (1994).
5. Percy, K. E. et al. Altered performance of forest pests under CO<sub>2</sub>- and O<sub>3</sub>-enriched atmospheres. *Nature* **420**, 403–407 (2002).
6. *Latest Findings on National Air Quality: 2002 Status and Trends* (US Environmental Protection Agency).
7. Findlay, S., Carreiro, M., Krischik, V. & Jones, C. G. Effects of damage to living plants on leaf litter quality. *Ecol. Appl.* **6**, 269–275 (1996).
8. Coleman, M. D., Dickson, R. E., Isebrands, J. G. & Karnosky, D. F. Carbon allocation and partitioning in aspen clones varying in sensitivity to tropospheric ozone. *Tree Physiol.* **15**, 593–604 (1995).
9. Andersen, C. P. Source-sink balance and carbon allocation below ground in plants exposed to ozone. *New Phytol.* **157**, 213–228 (2003).
10. King, J. S. et al. Fine-root biomass and fluxes of soil carbon in young stands of paper birch and trembling aspen as affected by elevated atmospheric CO<sub>2</sub> and tropospheric O<sub>3</sub>. *Oecologia* **128**, 237–250 (2001).
11. Dickson, R. E. et al. *Forest Atmosphere Carbon Transfer and Storage (FACTS-II)—The Aspen Free-air CO<sub>2</sub> and O<sub>3</sub> Enrichment (FACE) Project: An Overview* (Technical Report NC-214, USDA, Washington DC, 2000).
12. Leavitt, S. W., Follett, R. F. & Paul, E. A. Estimation of slow- and fast-cycling soil organic carbon pools from 6N HCl hydrolysis. *Radiocarbon* **38**, 231–239 (1996).
13. Paul, E. A. et al. Radiocarbon dating for determination of soil organic matter pool sizes and dynamics. *Soil Sci. Soc. Am. J.* **61**, 1058–1067 (1997).
14. Phillips, R., Zak, D. R., Holmes, W. E. & White, D. C. Microbial community composition and function beneath temperate trees exposed to elevated atmospheric carbon dioxide and ozone. *Oecologia* **131**, 236–244 (2002).
15. Larson, J., Zak, D. R. & Sinsabaugh, R. L. Extracellular enzyme activity beneath temperate trees growing under elevated carbon dioxide and ozone. *Soil Sci. Soc. Am. J.* **66**, 1848–1856 (2002).

**Acknowledgements** This research was supported by the US Department of Energy's Office of Science (BER: Program for Ecosystem Research and National Institute for Global Environmental Change), the USDA Forest Service (Northern Global Change and North Central Research Station), the National Science Foundation (DEB, DBI/MRI), and the USDA Natural Research Initiatives Competitive Grants Program. G. Hendry, K. Lewin, J. Nagey, D. Karnosky and J. Sober have been instrumental in the successful implementation of this long-term field experiment.

**Competing interests statement** The authors declare that they have no competing financial interests.

**Correspondence** and requests for materials should be addressed to W.M.L. (wmloya@mtu.edu).

**Flying and swimming animals cruise at a Strouhal number tuned for high-power efficiency**

Graham K. Taylor, Robert L. Nudds\* & Adrian L. R. Thomas

<sup>1</sup>Zoology Department, University of Oxford, Tinbergen Building, South Parks Road, Oxford OX1 3PS, UK

\* Present address: School of Biology, University of Leeds, L. C. Miall Building, Clarendon Way, Leeds LS2 9JT, UK

Dimensionless numbers are important in biomechanics because their constancy can imply dynamic similarity between systems, despite possible differences in medium or scale<sup>1</sup>. A dimensionless parameter that describes the tail or wing kinematics of swimming and flying animals is the Strouhal number<sup>1</sup>,  $St = fA/U$ , which divides stroke frequency (f) and amplitude (A) by forward speed (U)<sup>2–8</sup>. It is known to govern a well-defined series of vortex growth and shedding regimes for airfoils undergoing pitching and heaving motions<sup>6,8</sup>. Propulsive efficiency is high over a narrow range of St and usually peaks within the interval  $0.2 < St < 0.4$  (refs 3–8). Because natural selection is likely to tune animals for optimal propulsive efficiency, we expect it to constrain the range of St that animals use. This seems to be true for dolphins<sup>2–5</sup>, sharks<sup>3–5</sup> and bony fish<sup>3–5</sup>, which swim at  $0.2 < St < 0.4$ . Here we show that birds, bats and insects also converge on the same narrow range of St, but only when cruising. Tuning cruise kinematics to optimize St therefore seems to be a general principle of oscillatory lift-based propulsion.

Experiments with isolated pitching or heaving foils have measured extremely high peak propulsive efficiencies within the interval  $0.2 < St < 0.4$  (modal peak at  $St \approx 0.3$ )<sup>3–7</sup>. In this range, the propulsive efficiency (defined as the ratio of aerodynamic power output to mechanical power input) can be as high as 70% (ref. 7) or even 80% (ref. 6). Optimal St depends subtly on kinematic parameters including geometric angle of attack, amplitude-to-chord ratio, airfoil section and phase of motion<sup>6–8</sup> but, for any given motion, efficiency is usually high (>60%) over a range narrower than  $0.2 < St < 0.4$  (refs 3–7). For example, measured efficiency can plummet from 80% at  $St = 0.27$  to 10% at  $St = 0.09$  (ref. 6) and also drops off at higher St, albeit more gently<sup>7,8</sup>. Measured propulsive efficiency usually peaks when the kinematics result in maximum amplification of the shed vortices in the wake and an average velocity profile equivalent to a jet<sup>3,4,6</sup>.

Theoretical treatments of flapping wings<sup>3,4,6,8</sup> further confirm the empirical result that St tightly constrains propulsive efficiency. In fact, St is bound to affect aerodynamic force coefficients and propulsive efficiency, because it defines the maximum aerodynamic angle of attack and the timescales associated with the growth and shedding of vortices, which are the source of aerodynamic force production<sup>8,9</sup>. Natural selection is expected to favour wing kinematics that combine high propulsive efficiency with a high aerodynamic force coefficient. These need not peak at identical St, but can do for certain motions<sup>7,8</sup>: if not, selection should optimize the trade-off. Propulsive efficiency may be the more important selection pressure in cruising, whereas high aerodynamic force coefficients may be more important in accelerations, slow locomotion or hovering. In cruising flight or swimming, we therefore predict that St will be tuned for high propulsive efficiency.

This suggestion has already been made for cruising fish and dolphins<sup>2–5</sup>, which operate within the range  $0.2 < St < 0.4$ , and the principle is considered so general for swimming animals that it has even been used to predict the speeds of extinct ichthyosaurs<sup>10</sup>. Whereas the fluid dynamic results described above<sup>3–8</sup> refer to